EFDA–JET–CP(14)06/33

A.B. Kukushkin, V.S. Neverov, M.F. Stamp, A.G. Alekseev, S. Brezinsek, A.V. Gorshkov, M. von Hellermann, M.B. Kadomtsev, V. Kotov, A.S. Kukushkin, M.G. Levashova, S.W. Lisgo, V.S. Lisitsa, V.A. Shurygin, E. Veshchev, D.K. Vukolov, K.Yu. Vukolov and JET EFDA contributors

Theoretical Model of ITER High Resolution H-alpha Spectroscopy for a Strong Divertor Stray Light and Validation Against JET-ILW Experiments

Theoretical Model of ITER High Resolution H-alpha Spectroscopy for a Strong Divertor Stray Light and Validation Against JET-ILW Experiments

A.B. Kukushkin[1,2], V.S. Neverov[1], M.F. Stamp[3], A.G. Alekseev[1], S. Brezinsek[4], A.V. Gorshkov[1], M. von Hellermann[4], M.B. Kadomtsev[1], V. Kotov[4], A.S. Kukushkin[5], M.G. Levashova[1], S.W. Lisgo[5], V.S. Lisitsa[1], V.A. Shurygin[5], E. Veshchev[5], D.K. Vukolov[1], K.Yu. Vukolov[1] and JET EFDA contributors*

JET-EFDA, Culham Science Centre, OX14 3DB, Abingdon, UK

[1]National Research Centre "Kurchatov Institute", Moscow, 123182, Russia
[2]National Research Nuclear University MEPhI, Moscow, 115409, Russia
[3]EURATOM-CCFE Fusion Association, Culham Science Centre, OX14 3DB, Abingdon, OXON, UK
[4]Forschungszentrum Jülich, Euratom Association, Jülich, 52425, Germany
[5]ITER Organization, Route de Vinon-sur-Verdon, CS 90 046, 13067 St. Paul Lez Durance Cedex, France
** See annex of F. Romanelli et al, "Overview of JET Results",*
(25th IAEA Fusion Energy Conference, St Petersburg, Russia (2014)).

Preprint of Paper to be submitted for publication in Proceedings of the
25th IAEA Fusion Energy Conference, St Petersburg, Russia
13th October 2014 - 18th October 2014

Abstract
Theoretical model suggested for ITER H-alpha High-Resolution Spectroscopy (HRS) is validated against recent JET ITER-like wall (ILW) experiments. The model is aimed at reconstruction of neutral hydrogen isotopes density in the SOL, and isotope ratio, via solving a multi-parametric inverse problem with allowance for (i) a strong divertor stray light (DSL) on the main-chamber lines-of-sight (LoS), (ii) substantial deviation of neutral atom velocity distribution function from a Maxwellian in the SOL, (iii) data for direct observation of divertor. The developed "synthetic" Balmer-alpha diagnostic is tested on the example of data from the SOLPS4.3 (B2-EIRENE) code predictive modeling of the flat-top of Q=10 inductive operation of ITER. The JET-ILW HRS data on resolving the power at deuterium spectral line D-alpha with direct observation of the divertor from the top and with observation of the inner wall along tangential and radial LoS from equatorial ports are analyzed. These data allow to evaluate the spectrum of the DSL and the signal-to-background ratio for D- alpha light emitted from the far SOL and divertor in JET-ILW. The results support the expectation of a strong impact of the DSL upon the H-alpha (and Visible Light) Spectroscopy Diagnostic in ITER.

1. Introduction

The use of an all-metal first wall in future magnetic fusion reactors equipped with a divertor may impose severe limitations on the capabilities of optical diagnostics in the main chamber because of a divertor stray light (DSL) produced by multiple (diffusive and/or mirror) reflections of intense light emitted in the divertor. For optical diagnosis of hydrogen isotopes and various neutral and low ionized impurities in the far scrape-off layer (SOL) of the main chamber, one should expect strong contribution of the DSL in the same spectral lines. Preliminary analysis of the DSL problem for the H-alpha (and Visible Light) Spectroscopy Diagnostic in ITER suggested that there may be a substantial dominance of the Balmer-alpha DSL over the Balmer-alpha light emitted from the SOL (SOL light, SOLL), up to two orders of magnitude for highly reflecting walls and high-power operation. To meet the ITER measurement requirements, one needs to develop a detailed assessment of the measurement accuracy for the fuel ratio and the recycling flux from the main-chamber first wall. First results [1] have shown that a test of the elaborated approach in the currently running machines with all-metal first wall is required to benchmark the analysis method.

Here, we report on the validation of essential features of theoretical model, suggested for ITER H-alpha High-Resolution Spectroscopy (HRS), against recent JET ITER-like wall (ILW) experiments. The model is aimed at reconstruction of the neutral hydrogen isotopes density in the SOL, together with the isotope ratio, via solving a multi-parametric inverse problem with allowance for (i) a strong DSL on the main-chamber lines-of-sight (LoS), (ii) substantial deviation of the neutral atom velocity distribution function (VDF) from a Maxwellian in the SOL, (iii) data from direct observation of the divertor. The bifurcated-LoS measurement scheme [1] suggested for ITER (namely, targeting at an optical dump and very close to it) cannot be tested now on JET for technical reasons. The main goal of the present validation is to evaluate the accuracy of recovering the DSL/SOLL ratio.

2. Theoretical Model

The formalism of inverse problem uses semi-analytic models: (a) the model [1] for the DSL spectral line shape, extended to allow for angle anisotropy of the DSL, and (b) a model for the spectral line shape asymmetry caused by the inward flux of relatively fast atoms. The latter model is suggested by the results of the 1D model [2,3] for neutral atom VDF in the SOL, tested against the EIRENE code stand-alone simulations of neutral deuterium VDF, applied on the plasma background calculated by the SOLPS4.3 (B2-EIRENE) code [4-6].

The first component of the algorithm is the recovery of the spatial distribution of neutral atom temperature along each track of observation from the top of main chamber down to the divertor. Spatial profile along each LoS (track) is approximated by a histogram with a small number (M) of possible values of temperature (typically 3: a "cold", "warm" and "hot" component). Here we solve an inverse problem for each track of the spectrometers for each time moment ("time moment" designates the time interval, of a certain exposure, during which the collected photons are counted) which, e.g., for deuterium working gas with hydrogen admixture, has the form:

$$\sum_{j=1}^{N_{tr}}\left(\tilde{S}_{tr}^{exp}(\lambda_j)-\left\{\sum_{i=1}^{M}x_{tr}^{(i)}\frac{1}{F_{sum}(T_{tr}^{(i)},C_{H,tr})}\begin{pmatrix}F_{Gauss}(\lambda_j-\lambda_{Da},T_{tr}^{(i)})\\+C_{H,tr}F_{Gauss}(\lambda_j-\lambda_{Ha},T_{tr}^{(i)})\end{pmatrix}\right\}\right)^2\xrightarrow[\mathbf{x}_{tr},\,\mathbf{T}_{tr},C_{H,tr}]{}min,\qquad(1)$$

$$tr=1{:}\,Tr_{max}^{div}.$$

Here the input parameters are: (i) N_{tr} the number of spectral channels (pixels) on the track number tr in the spectral range selected for analysis (e.g., the π-component of the Zeeman spectrum is sufficient in this step); (ii) $\tilde{S}_{tr}^{exp}$ the normalized experimental spectrum measured on the track number tr: $\tilde{S}_{tr}^{exp}(\lambda_j)=\frac{S_{tr}^{exp}(\lambda_j)}{\sum_{j=1}^{N_{tr}^{total}}S_{tr}^{exp}(\lambda_j)}$, where S_{tr}^{exp} is the experimental spectrum and N_{tr}^{total} is the total number of pixels on the track number tr in the spectral range of D+H Balmer-alpha lines including the broad wings of the line shape (N_{tr}^{total} can be greater than N_{tr}), j is the pixel index; (iii) Tr_{max}^{div} the number of the divertor observation tracks and (iv) M the number of the temperature values to be recovered. Here F_{Gauss} is the Gaussian function,

$$F_{sum}(T_{tr}^{(i)},C_{H,tr})=\sum_{j=1}^{N_{tr}^{total}}\left(F_{Gauss}(\lambda_j-\lambda_{Da},T_{tr}^{(i)})+C_{H,tr}F_{Gauss}(\lambda_j-\lambda_{Ha},T_{tr}^{(i)})\right);$$

and λ_{Da}, λ_{Ha} are the deuterium Balmer-alpha (656.1 nm) and hydrogen Balmer-alpha (656.28 nm) wavelengths. The output parameters (i.e. those to be recovered) are: (i) $T_{tr}^{(i)}$, the temperature of the i-th fraction of atoms on the track number tr, (ii) $x_{tr}^{(i)}$, the partial contribution of the i-th fraction of atoms to the intensity measured on the track number tr and (iii) $C_{H,tr}$, the contribution of hydrogen atoms emissivity to the measured intensity, namely the H/D ratio for the track number tr.

The second component of the algorithm is the evaluation of the DSL spectrum using the data from the direct observation of the divertor. The (normalized) line shape of the DSL spectrum is calculated as follows:

$$S_{DSL}(\lambda)=\sum_{tr=1}^{Tr_{max}^{DSL}}\frac{S_{tr}\cdot R_{tr}}{S_{total}}\sum_{i=1}^{M}\hat{x}_{tr}^{(i)}\left(\begin{array}{c}\mathrm{C}_{\pi}^{(DSL)}F_{Gauss}(\lambda-\lambda_{Da},\hat{T}_{tr}^{(i)})\\+\frac{(1-\mathrm{C}_{\pi}^{(DSL)})}{2}\begin{Bmatrix}F_{Gauss}(\lambda-\lambda_{Da}-\Delta\lambda_{D,tr}^{Zeem}(R_{tr}),\hat{T}_{tr}^{(i)})\\+F_{Gauss}(\lambda-\lambda_{Da}+\Delta\lambda_{D,tr}^{Zeem}(R_{tr}),\hat{T}_{tr}^{(i)})\end{Bmatrix}\\+\hat{C}_{H,tr}\mathrm{C}_{\pi}^{(DSL)}F_{Gauss}(\lambda-\lambda_{Ha},\hat{T}_{tr}^{(i)})\\+\hat{C}_{H,tr}\frac{(1-\mathrm{C}_{\pi}^{(DSL)})}{2}\begin{Bmatrix}F_{Gauss}(\lambda-\lambda_{Ha}-\Delta\lambda_{H,tr}^{Zeem}(R_{tr}),\hat{T}_{tr}^{(i)})\\+F_{Gauss}(\lambda-\lambda_{Ha}+\Delta\lambda_{H,tr}^{Zeem}(R_{tr}),\hat{T}_{tr}^{(i)})\end{Bmatrix}\end{array}\right),\qquad(2)$$

where S_{tr} is the wavelength-integrated intensity on the track number tr and R_{tr} is the major radius of the point of maximum emissivity on the given track. Here the $S_{tr}\cdot R_{tr}$ product recalculates the observation volume of the given track to the volume of the respective emitting toroidal ring. S_{total} is the total intensity of the divertor emission: $S_{total}=\sum_{tr=1}^{Tr_{max}^{DSL}}S_{tr}\cdot R_{tr}$; Tr_{max}^{DSL} is the number of tracks used to calculate the DSL; $\hat{x}_{tr}^{(i)}$, $\hat{T}_{tr}^{(i)}$ and $\hat{C}_{H,tr}$ are the values of partial contributions, temperatures and H/D ratios, found by solving Eq. (1); $\Delta\lambda_{tr}^{Zeem}(R_{tr})$ is the Zeeman splitting for the track number tr, calculated for magnetic field at the point R_{tr} (we allow for toroidal field only); $\mathrm{C}_{\pi}^{(DSL)}$ is the partial contribution of the Zeeman π-component to the total line shape (this is an optimization parameter varied in the range:

$0.15 \le C_{\pi}^{(DSL)} \le 0.5$, where upper bound corresponds to the case of emission only transverse to magnetic field; in the model [1] of uniform spatial and angle distribution of the DSL intensity one has $C_{\pi}^{(DSL)} = 0.25$; the variation allows for deviation of the DSL intensity from the above uniformity).

The third component of the algorithm is the recovery of the main parameters of the non-Maxwellian velocity distribution function (VDF) of neutral atoms in the SOL. The inverse problem is similar to Eq. (1) where the theoretical spectrum is taken in the following form:

$$S_{SOL}^{model} = \sum_{m=1}^{M1} x_M^{(m)} \left(F_{Maxw}^{SOL}\left(\lambda, \Delta\lambda_D^{Zeem}, \lambda_{Da}, C_\pi, T_M^{(m)}\right) + C_H F_{Maxw}^{SOL}\left(\lambda, \Delta\lambda_H^{Zeem}, \lambda_{Ha}, C_\pi, T_M^{(m)}\right)\right) + \sum_{n=1}^{M2} x_N^{(n)} \left(F_{Non-Maxw}^{SOL}\left(\lambda, \Delta\lambda_D^{Zeem}, \lambda_{Da}, C_\pi, T_N^{(n)}, \Lambda^{(n)}\right) + C_H F_{Non-Maxw}^{SOL}\left(\lambda, \Delta\lambda_H^{Zeem}, \lambda_{Ha}, C_\pi, T_N^{(n)}, \Lambda^{(n)}\right)\right), \quad (3)$$

$$F_{Maxw}^{SOL}\left(\lambda, \Delta\lambda_D^{Zeem}, \lambda_{Da}, C_\pi, T_M^{(m)}\right) = C_\pi F_{Gauss}\left(\lambda - \lambda_{Da}, T_M^{(m)}\right) + \frac{(1 - C_\pi)}{2}\left(F_{Gauss}\left(\lambda - \Delta\lambda^{Zeem} - \lambda_{Da}, T_M^{(m)}\right) + F_{Gauss}\left(\lambda + \Delta\lambda^{Zeem} - \lambda_{Da}, T_M^{(m)}\right)\right), \quad (4)$$

$$F_{Non-Maxw}^{SOL}\left(\lambda, \Delta\lambda_D^{Zeem}, \lambda_{Da}, C_\pi, T_N^{(n)}, \Lambda^{(n)}\right) = C_\pi F_{Gauss}\left(\lambda - \lambda_{Da}, T_N^{(n)}\right) exp\left(-\frac{\Lambda^{(n)}}{|\lambda - \lambda_{Da}|}\right)\eta\left((\lambda_{Da} - \lambda)(\mathbf{k}.\mathbf{l})\right) + \frac{(1 - C_\pi)}{2}\left(\begin{array}{l} F_{Gauss}\left(\lambda - \Delta\lambda^{Zeem} - \lambda_{Da}, T_N^{(n)}\right) \exp\left(-\frac{\Lambda^{(n)}}{|\lambda - \Delta\lambda^{Zeem} - \lambda_{Da}|}\right)\eta\left((\lambda_{Da} - \lambda + \Delta\lambda^{Zeem})(\mathbf{k}.\mathbf{l})\right) \\ + F_{Gauss}\left(\lambda + \Delta\lambda^{Zeem} - \lambda_{Da}, T_N^{(n)}\right) exp\left(-\frac{\Lambda^{(n)}}{|\lambda + \Delta\lambda^{Zeem} - \lambda_{Da}|}\right)\eta\left((\lambda_{Da} - \lambda - \Delta\lambda^{Zeem})(\mathbf{k}.\mathbf{l})\right) \end{array}\right). \quad (5)$$

Here the input (known) parameters are: (i) $M1$ and $M2$ – the numbers of, respectively, the Maxwellian and non-Maxwellian fractions of the VDF for the neutral atoms; (ii) $F_{Maxw}^{SOL}\left(\lambda_j, \Delta\lambda_D^{Zeem}, \lambda_{Da}, C_\pi, T_M^{(m)}\right)$ and $F_{Non-Maxw}^{SOL}\left(\lambda_j, \Delta\lambda_D^{Zeem}, \lambda_{Da}, C_\pi, T_N^{(n)}, \Lambda^{(n)}\right)$ – the contributions of the abovementioned Maxwellian and non-Maxwellian fractions of the VDF to the spectrum, respectively; (iii) $\Delta\lambda^{Zeem}$ – the Zeeman splitting, calculated for magnetic field at the point of maximum emissivity within the emitting layer of the SOL plasma (we allow for toroidal field only) and (iv) C_π – the partial contribution of the Zeeman π-component to the total line shape calculated for the above-mentioned value of the magnetic field. $\eta(\mathrm{x})$ is the Heaviside function, **k** is the direction of atomic flux from the nearest part of the wall to the plasma and **l** is the LoS direction (from the detector to the observation point). The output (unknown) parameters are: (i) $T_M^{(m)}$ – the temperature of the *m*–th Maxwellian group of deuterium atoms; (ii) $T_N^{(n)}$ – the effective temperature of the *n*-th non-Maxwellian group of deuterium atoms; (iii) $x_{M\,\{N\}}^{(m)\{(n)\}}$ – the statistical weight of the contribution of the *m*-th Maxwellian (*n*-th non-Maxwellian) group to the total intensity of the line; (iv) $\Lambda^{(n)}$ – the characteristic wavelength shift for the spectral contribution of the *n*-th group of non-Maxwellian atoms which describes the attenuation of the inward flux (a description of the model for the asymmetry of the line shapes, including the introduction of the damping factors with $\Lambda^{(n)}$, is given in [7]) and (v) C_H – the contribution of hydrogen atom emissivity to the measured intensity, actually the H/D ratio.

The above-mentioned three components are combined in the final inverse problem which takes into account all possible sources of the detected signal: the DSL and the two emitting plasma layers in the SOL along the LoS in the main chamber, namely, near the inner wall limiter ("inner SOL") and the outer wall limiter ("outer SOL"). We introduce the following simplifications to the model: (i) the H/D ratio, C_H, is the same in the outer and inner SOL and (ii) the effective temperatures of non-Maxwellian fractions are equal to the temperatures of the respective Maxwellian "warm" and "hot" fractions: $T_N^{(n)} = T_M^{(n+1)}, n = 1, 2$. The inverse problem is formulated as follows:

$$\sum_{j=1}^{N}\left(\begin{array}{c}\tilde{S}_{tr}^{[SOL]\,exp}(\lambda_j)-x_{tr}^{DSL}\tilde{S}_{DSL}\left(\mathrm{C}_{\pi,tr}^{(DSL)},\lambda_j\right)\\ -\sum_{p=1}^{2}\left\{\begin{array}{c}\sum_{i=1}^{M}x_{tr,p}^{(i)}\frac{1}{(F_M^{sum})_{tr,p}^{(i)}}\left(\begin{array}{c}F_{Maxw}^{SOL}\left(\lambda_j,\Delta\lambda_{Da,tr,p}^{Zeem},\lambda_{Da},\mathrm{C}_{\pi,tr,p}^{(SOL)},T_{tr,p}^{(i)}\right)\\ +C_{H,tr}F_{Maxw}^{SOL}\left(\lambda_j,\Delta\lambda_{Ha,tr,p}^{Zeem},\lambda_{Ha},\mathrm{C}_{\pi,tr,p}^{(SOL)},T_{tr,p}^{(i)}\right)\end{array}\right)\\ +\sum_{i=2}^{M}x_{tr,p}^{(M+i)}\frac{1}{(F_N^{sum})_{tr,p}^{(i)}}\left(\begin{array}{c}F_{Non-Maxw}^{SOL}\left(\lambda_j,\Delta\lambda_{Da,tr,p}^{Zeem},\lambda_{Da},\mathrm{C}_{\pi,tr,p}^{(SOL)},T_{tr,p}^{(i)},\Lambda_{tr,p}^{(i)}\right)\\ +C_{H,tr}F_{Non-Maxw}^{SOL}\left(\lambda_j,\Delta\lambda_{Ha,tr,p}^{Zeem},\lambda_{Ha},\mathrm{C}_{\pi,tr,p}^{(SOL)},T_{tr,p}^{(i)},\Lambda_{tr,p}^{(i)}\right)\end{array}\right)\end{array}\right\}\end{array}\right)^2 \xrightarrow[\substack{\mathrm{C}_{\pi,tr}^{(DSL)},\\ \mathbf{x}_{tr},\mathbf{T}_{tr},\\ \mathbf{\Lambda}_{tr},C_{H,tr}}]{} min, \tag{6}$$

$$(F_M^{sum})_{tr,p}^{(i)}=\sum_{j=1}^{N_{tr}^{total}}\left(F_{Maxw}^{SOL}(\lambda_j,\dots)+C_{H,tr}F_{Maxw}^{SOL}(\lambda_j,\dots)\right),$$

$$(F_N^{sum})_{tr,p}^{(i)}=\sum_{j=1}^{N_{tr}^{total}}\left(F_{Non-Maxw}^{SOL}(\lambda_j,\dots)+C_{H,tr}F_{Non-Maxw}^{SOL}(\lambda_j,\dots)\right),\qquad tr=1{:}\,Tr_{max}^{SOL},$$

where the p subscript indicates that the parameter can have different values for the inner and outer sections of the SOL which contribute to the given track, $\tilde{S}_{tr}^{[SOL]exp}$ is the normalized experimental spectrum measured on the SOL-directed track number tr, $\tilde{S}_{tr}^{[SOL]exp}(\lambda_j)=S_{tr}^{[SOL]exp}(\lambda_j)/(\sum_{j=1}^{N_{tr}^{total}}S_{tr}^{[SOL]exp}(\lambda_j))$, where $S_{tr}^{[SOL]exp}$ is the experimental spectrum and N_{tr}^{total} is the total number of pixels on the track number tr in the spectral range of D+H Balmer-alpha lines, including the broad wings of the line shape; Tr_{max}^{SOL} is the number of SOL observation tracks; $\tilde{S}_{DSL}$ is the normalized DSL spectrum, $\sum_{j=1}^{N_{tr}^{total}}\tilde{S}_{DSL}\left(\mathrm{C}_{\pi,tr}^{(DSL)},\lambda_j\right)=1$; x_{tr}^{DSL} is the unknown fraction of the DSL in the measured signal.

We assume also that the DSL/signal ratio for the LoS in the main chamber (DSL/SOLL ratio) should be proportional to the ratio of the total power of divertor emission to the SOLL intensity with the proportionality coefficient which only depends on the geometrical parameters and is independent on time. The validity of this assumption is based either on the possibility to treat the divertor as a localized source of the DSL, or (which is less likely) on the time independence of the spatial profile (not of the absolute value) of the emission source. This constant may be evaluated for each LoS in the main chamber via averaging over time within many pulses. Thus, in the final algorithm we use the correlation between the DSL fraction in the signal on the tracks in the main chamber and the intensity of the divertor emission observed directly. This enables us to increase the accuracy of the recovery of the DSL/SOLL ratio.

The third component of the developed "synthetic" Balmer-alpha spectroscopy diagnostic was tested on the example of data from predictive modeling of the flat-top of Q=10 inductive operation of ITER, with account of the poloidally resolved plasma recycling from the FW in the framework of the "extended grid" approach [8]. Tables 1 and 2 in [9] show reasonably good agreement between the LoS-average results for the temperatures (the effective ones for non-Maxwellian fractions of VDF) from the EIRENE simulations and those recovered from the developed algorithm which originally operates with the LoS-average parameters. A more detailed comparison is given in [10].

3. Validation of the Model Against JET-ILW Experiments

We analyze high-resolution spectrometer data on resolving the power in Balmer-alpha deuterium and hydrogen spectral lines from direct observation of the divertor from the top (KSRB Tracks 1-10 and KSRD Tracks 1-10 covering, respectively, the outer and inner divertors; the Zeeman σ-components are filtered out; spectral resolution 0.0521 and 0.522 A/pixel) and the observation of the inner wall from equatorial ports (KSRB Track 11 is a

radial line-of-sight (LoS) at the vertical coordinate Z= ~ +200 mm, targeted at a 200 mm spot which covers partly the inboard poloidal limiter and partly the inner wall cladding tile in the 8th octant; KSRB Track 12 is a tangential LoS at Z=~0, targeted at a similar spot at one side of a beryllium inboard poloidal limiter in the 7th octant, with the angle between the LoS and toroidal field at inner wall Φ =~35.5^o).

We show typical results in the figures for the two pulses: JET Pulse Number (JPN) 85844 and JPN 86413 with moderate (~ 11 MW) and high power (~ 23 MW) NBI, respectively. The latter pulse is characterized by a relatively high content of hydrogen in the H+D mixture. Figure 1 shows fitting of the spectra on the KSRB tracks 11 and 12 for the divertor stage of the JPN 85844 (at time t = 10.05 s) in the case of M = 3 in Eq. (6). Note that the red wings of the spectrum in Figure 1 are broader than the blue ones. In our model such an asymmetry may be interpreted only as being caused by the contribution of the light from the outer section of the LoS in the SOL. The optimal value of the objective function (minimized in Eq. 6) for the KSRB Track 11 is ten times lower than that for the KSRB Track 12 because of the factor ten stronger signal on the Track 11. Figures 2 and 3 show the time dependence of partial contributions of the various sources of the signal (inner-wall SOL, outer-wall SOL, DSL) to the integral intensity for the KSRB tracks 11 and 12 for JPN 85844 and 86413, respectively.

The signal on the Track 12 is weak. The weaker is the signal the larger is the spread of the recovered values. Figure 4 shows the time dependence of the H/(H+D) ratio in the divertor and SOL, recovered for JPN 86413. The recovered values of the H/(H+D) ratio are almost the same in the SOL and divertor and vary from 0.05 to 0.15. Figure 5 shows the time dependence of main parameters of this discharge.

4. Discussion, Conclusions

The deuterium and hydrogen Balmer-alpha line high-resolution spectroscopy (HRS) data from JET-ILW experiments are interpreted with the algorithms developed for the H-alpha (and Visible Light) Spectroscopy Diagnostic in ITER. This enabled us to evaluate (i) the shapes of the spectra of the light emitted from the far SOL (SOL light, SOLL) and divertor, both observed directly and as a divertor stray light (DSL) on the lines of sight (LoS) in the main chamber, and (ii) the ratio of respective total intensities (SOLL/DSL). The recovery of the neutral atom density in the SOL can be done with the developed algorithm provided the absolute calibration of all the signals is available.

The uncertainty of the results for the DSL/SOLL is caused mainly by the closeness of the spectral shape of the SOLL from the outer-wall SOL to that of the DSL. The uncertainty is appreciably reduced thanks to assumption that the DSL/SOLL ratio should be proportional to the ratio of the total power of divertor emission to the intensity measured on the LoS in the main chamber with a proportionality coefficient which depends on the geometrical parameters only and is independent of time. This enabled us to recover the respective constant from data for many pulses, improve the stability of solving the inverse problems and thus decrease the noise of the results for the DSL/SOLL ratio by several times.

Our analysis of the discharges in the recent 2012 - 2013 campaign on JET-ILW, with intense emission from divertor magnetic, show the DSL/SOLL ratio to vary from ~2 to ~5 if neglecting the outer-wall SOLL, and from ~1 to ~2 if allowing for it, in moderate-power diverted discharge (JPN 83624, NBI ~12 MW). Similar results are obtained for high-power diverted discharge (JPN 83551, NBI ~25 MW) [9]. For the JPN 85831, 85843, 85845, 85847, 85848, 85853, 85854, 85855, 85859 and 85883 (NBI ~ 9-13 MW) in the last campaign, the DSL/SOLL, with account of outer-wall SOL and improved algorithm, is ~0.1-0.4 for the

KSRB track 11 (radial LoS) and ~ 0.25-0.6 for the KSRB track 12 (tangential LoS) at the high-power divertor stages of the discharges. The peak values ever attained during the essential part of the last campaign (JPN 85752 – 86451) are found to be ~0.7, for the track 11, and 1.5, for the track 12. More analysis is needed to identify the dependence of the DSL/SOLL on the divertor radiation power, recycling level, degree of detachment, divertor configuration, etc.

Thus, the results for the JET-ILW support the expectation of a strong impact of the DSL upon the H-alpha (and Visible Light) Spectroscopy Diagnostic in ITER. In ITER, for an expected stronger DSL, we plan to diminish the uncertainty of recovery of the SOLL and DSL by using the bifurcated-LOS measurements (targeting at an optical dump and very close to it) [1]. The validation of the bifurcated-LOS scheme in JET-ILW experiments would be very helpful for all ITER diagnostics in the visible light range.

The results show the importance of non-Maxwellian effects (and respective asymmetry of the line shape) in the interpretation of the Balmer-alpha high-resolution spectroscopy (HRS) data. This suggest that, on top of the methods based on the wavelength-integrated intensity (like the widely used S/XB method [11]), also the Balmer-alpha HRS is required to contribute to the technique for evaluation of the recycling flux from the main-chamber first wall.

Acknowledgements
This work was supported by the RF State Corporation ROSATOM and EURATOM, and carried out within the framework of the European Fusion Development Agreement.

Disclaimer: The views and opinions expressed herein do not necessarily reflect those of the European Commission and ITER Organization.

References

[1]. Kukushkin, A.B., et al. Proceedings 24th IAEA FEC, San Diego, USA, 8–13 October 2012, ITR/P5-44.
[2]. Kadomtsev, M.B., Kotov, V., Lisitsa, V.S., Shurygin, V.A., Proceedings 39th EPS Conference & 16th International Congress on Plasma Physics, Stockholm, Sweden, 2–6 July 2012, P4.093, http://ocs.ciemat.es/epsicpp2012pap/pdf/P4.093.pdf.
[3]. Lisitsa, V.S., et al. Atoms **2(2)** (2014) 195-206, doi:10.3390/atoms2020195.
[4]. Kukushkin, A.S., Pacher, H.D., Loarte, A., Kotov, V., et al. Nuclear Fusion, **49** (2009) 075008.
[5]. Braams, B.J. Computational studies in tokamak equilibrium and transport, PhD thesis. Utrecht: Rijksuniversitet, 1986.
[6]. Reiter, D., Baelmans, M., Börner, P., Fusion Science and Technology, **47** (2005) 172 (www.eirene.de).
[7]. Kukushkin, A.B., Neverov, V.S., et al. Proceedings 22nd ICSLS, Tullahoma, TN, USA, 1–6 June 2014 (to be published in Journal of Physics: Conference Series).
[8]. Lisgo, S.W., Börner, P., et al., Journal of Nuclear Materials **415** (2011) S965.
[9]. Kukushkin, A.B., Neverov, V.S., Stamp, M.F., et al., AIP Conference Proceedings **1612** (2014) 97.
[10]. Neverov, V.S., et al. Plasma Physics Reports, **41**, issue 2 (2015).
[11]. Bogen, P., Hartwig, H.H., Hintz, E., Hőthker, K., Lie, Y.T., Pospieszczyk, A., Samm, U., Bieger, W., Journal of Nuclear Materials **128–129** (1984) 157.

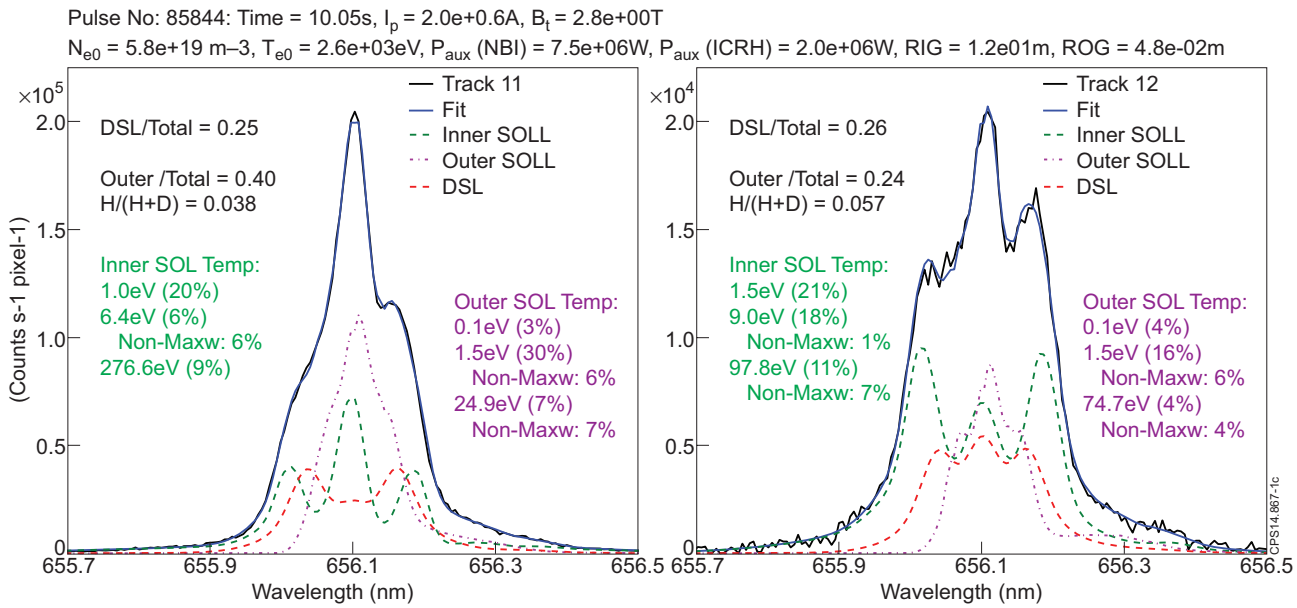

Figure. 1: The results of fitting the spectra on the KSRB tracks 11 (left) and 12 (right) for the divertor stage of the JET Pulse Number: 85844 (at time t = 10.05s). The temperatures of atomic fractions and partial contributions of fractions to the total intensity are indicated for both parts of the SOL plasma on the LoS. For moderate and high temperature fractions partial contributions of non-Maxwellian atoms to the total intensity are indicated. Ne0 and Te0 are the electron density and electron temperature values on the magnetic axis (High Resolution Thomson Scattering), RIG and ROG are the gaps between the separatrix and the inner and outer limiters respectively (EFIT code), Paux is auxiliary heating power.

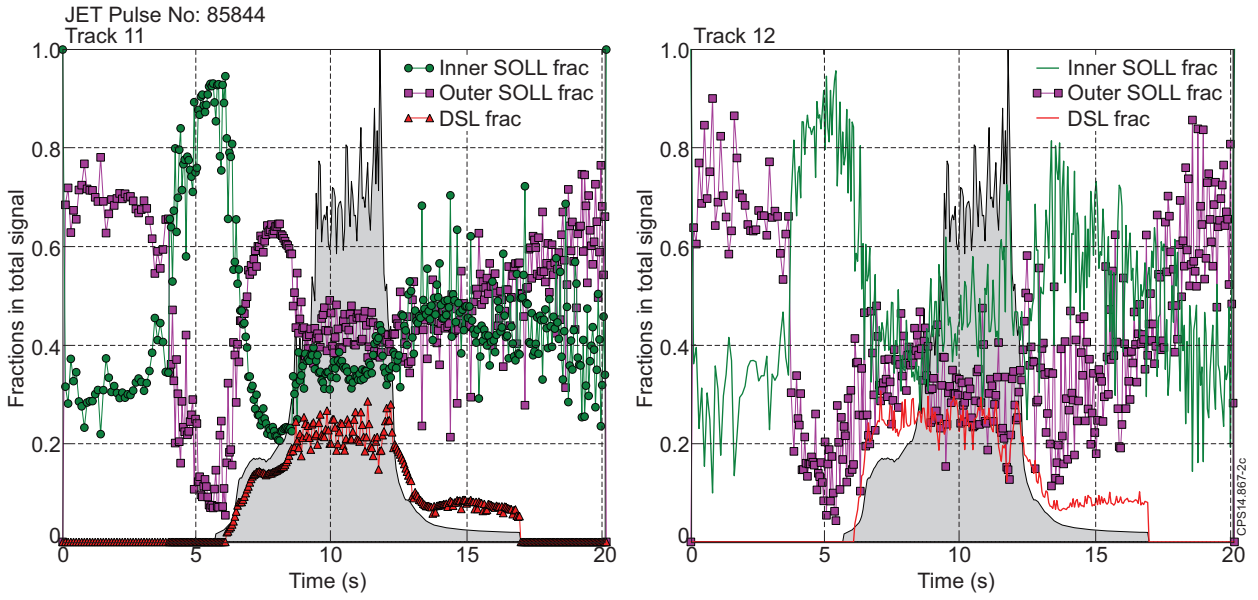

Figure 2: Time dependence of partial contributions of various sources of light (inner-wall SOL, outer-wall SOL, DSL) to the integral intensity for the KSRB tracks 11 and 12 for JET Pulse Number: 85844. The volume-integrated normalized H+D Balmer-alpha emission from the divertor is shown with grey background.

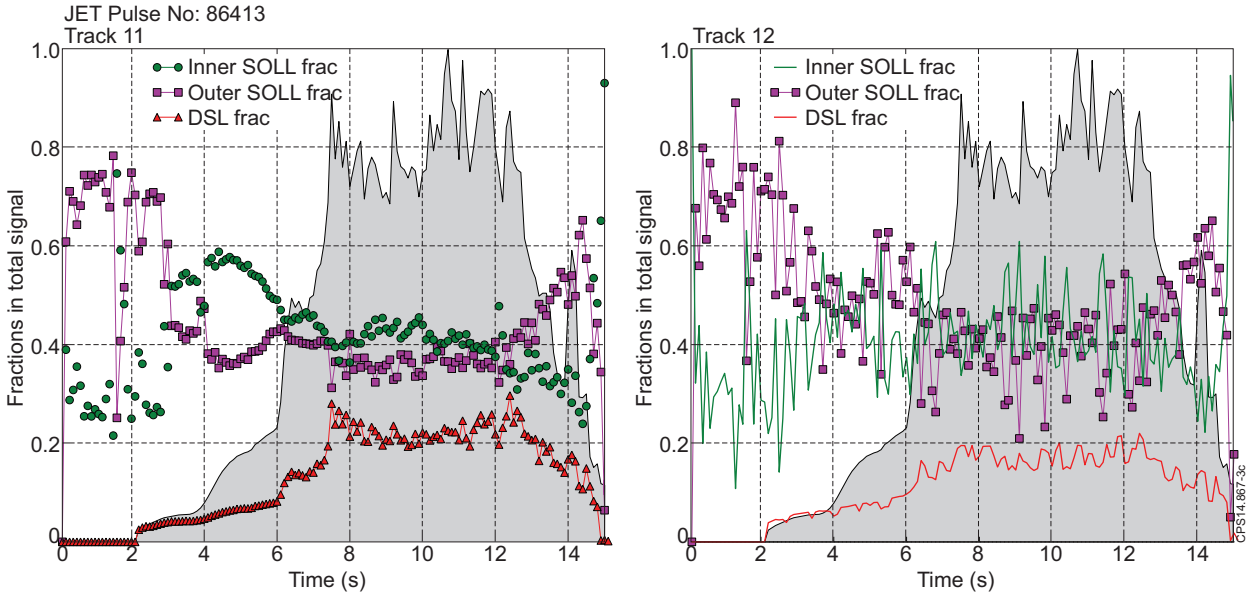

Figure 3: The same as in Figure 2 but for JET Pulse Number: 86413.

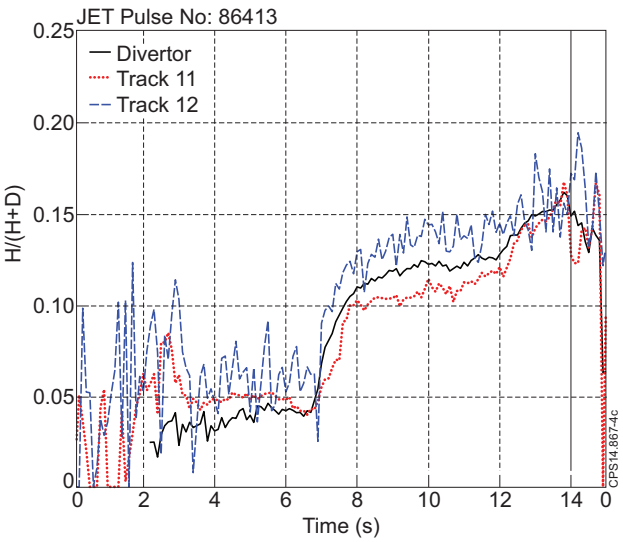

Figure 4: Time dependence of the H/(H+D) ratio in the divertor (volume averaged using the KSRB and KSRD divertor direct observation data) and in the SOL (KSRB tracks 11 and 12), recovered for JET Pulse Number: 86413.

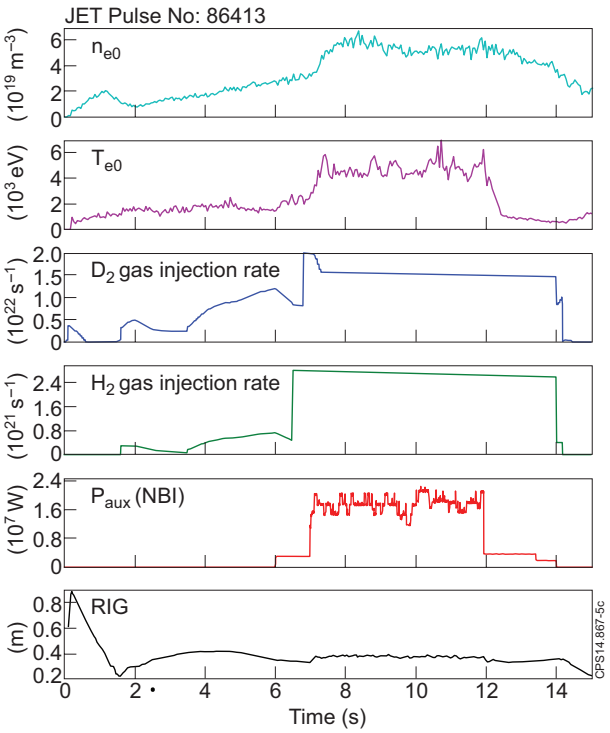

Figure 5: Time dependence of main parameters for JET Pulse Number: 86413, including the D_2 and H_2 gas injection rates (for other notations see Figure 1).